

Broad band polarimetric follow-up of Type IIP SN 2012aw

Brajesh Kumar^{1,2} \star , S. B. Pandey¹, C. Eswaraiah^{1,3}, J. Gorosabel^{4,5,6}

¹*Aryabhata Research Institute of Observational Sciences, Manora Peak, Nainital 263 002, India*

²*Institut d'Astrophysique et de Géophysique, Université de Liège, Allée du 6 Août 17, Bât B5C, 4000 Liège, Belgium*

³*Institute of Astronomy, National Central University, 300 Zhongda Rd, Zhongli, Taoyuan Country 32054, Taiwan*

⁴*Instituto de Astrofísica de Andalucía (CSIC), Glorieta de la Astronomía s/n, 18008 Granada, Spain*

⁵*Unidad Asociada Grupo Ciencia Planetarias UPV/EHU-IAA/CSIC, Departamento de Física Aplicada I, E.T.S. Ingeniería, Universidad del País Vasco UPV/EHU, Alameda de Urquijo s/n, E-48013 Bilbao, Spain*

⁶*Ikerbasque, Basque Foundation for Science, Alameda de Urquijo 36-5, E-48008 Bilbao, Spain.*

Accepted ———, Received ———; in original form ———

ABSTRACT

We present the results based on *R*-band polarimetric follow-up observations of the nearby (~ 10 Mpc) Type II-plateau SN 2012aw. Starting from ~ 10 days after the SN explosion, these polarimetric observations cover ~ 90 days (during the plateau phase) and are distributed over 9 epochs. To characterize the Milky Way interstellar polarization (ISP_{MW}), we have observed 14 field stars lying in a radius of 10° around the SN. We have also tried to subtract the host galaxy dust polarization component assuming that the dust properties in the host galaxy are similar to that observed for Galactic dust and the general magnetic field follow the large scale structure of the spiral arms of a galaxy. After correcting the ISP_{MW} , our analysis infer that SN 2012aw has maximum polarization of $0.85\% \pm 0.08\%$ but polarization angle does not show much variation with a weighted mean value of $\sim 138^\circ$. However, if both ISP_{MW} and host galaxy polarization (ISP_{HG}) components are subtracted from the observed polarization values of SN, maximum polarization of the SN becomes $0.68\% \pm 0.08\%$. The distribution of Q and U parameters appears to follow a loop like structure. The evolution of polarimetric light curve (PLC) properties of this event is also compared with other well studied core-collapse supernovae of similar type.

Key words: Supernovae: general – supernovae, polarimetry: individual – SN2012aw, galaxies: individual – NGC 3551

1 INTRODUCTION

Core-collapse supernovae (CCSNe) exhibit significant level of polarization during various phases of their evolution at optical/infrared wavelengths. In general, the degree of polarization of different types of SNe seems to increase with decreasing mass of the stellar envelope at the time of explosion (see Wheeler, 2000; Leonard et al., 2001; Wang et al., 2001; Leonard & Filippenko, 2005). Type II SNe are polarized at level of $\sim 1\% - 1.5\%$. However, Type Ib/c SNe (also known as stripped-envelope SNe as the outer envelopes of hydrogen and/or helium of their progenitors are partially or completely removed before the explosion) demonstrate significantly higher polarization in comparison to Type II SNe (for more details, see Leonard & Filippenko, 2001; Kawabata et al., 2002, 2003; Wang et al., 2003a; Gorosabel et al., 2006; Maund et al., 2007; Patat et al., 2012; Tanaka et al., 2012; Maund et al., 2013, and references therein). The higher polarization values observed in case of Type Ib/c SNe most probably arise due

to extreme departure from the spherical symmetry (Chugai, 1992; Höflich et al., 2001; Khokhlov & Höflich, 2001).

Theoretical modelling predicts that in general CCSNe show the degree of asymmetry of the order of $10\% - 30\%$ if modelled in terms of oblate/prolate spheroids (e.g. Hoflich, 1991). Numerical simulations (see Kasen et al., 2006; Dessart & Hillier, 2011) indicate that in case of Type II SNe, the level of polarization is also influenced by SN structure (e.g., density and ionization), apart from their initial mass and rotation. The possible progenitors of Type IIP SNe are low-mass red/blue super-giants and their polarization studies are extremely useful to understand the SN structure in detail. In spite of being the most common subtypes among the known CC-SNe, polarization studies of Type IIP SNe have been done only in a handful of cases (e.g. Barrett, 1988; Leonard et al., 2001, 2006; Leonard & Filippenko, 2001; Chugai, 2006; Chornock et al., 2010; Leonard et al., 2012a). In general, intrinsic polarization in these SNe are observed below 1% but few exceptions exist in literature (for example Chornock et al. (2010) reported $\sim 1.5\%$ for SN 2006ov).

\star E-mail: brajesh@aries.res.in, brajesharies@gmail.com

Systematic polarimetric studies have been started, only after

the observations of Type IIP SN 1987A (see Cropper et al., 1988; Mendez et al., 1988; Jeffery, 1991). Shapiro & Sutherland (1982) first pointed out that polarimetry provides direct powerful probe to understand the SN geometry (see also McCall, 1984; Hoefflich, 1991). Polarization is believed to be produced due to electron scattering within the SN ejecta. When light passes through the expanding ejecta of CCSNe, it retains information about the orientation of layers. In spherically symmetric scenario, the equally present directional components of the electric vectors will be canceled out to produce zero net polarization. If the source is aspherical, incomplete cancellation occurs which finally imprint a net polarization (see Fig. 1 of Filippenko & Leonard 2004 and Leonard & Filippenko 2005). In addition to asphericity of the electron scattering atmosphere, there are several other processes which can produce polarization in CCSNe such as scattering by dust (e.g. Wang & Wheeler, 1996); clumpy ejecta or asymmetrically distributed radioactive material within the SN envelope (e.g. Hoefflich, 1995; Chugai, 2006), and aspherical ionization produced by hard X-rays from the interaction between the SN shock front and a non-spherical progenitor wind (Wheeler & Filippenko, 1996).

To diagnose the underlying polarization in SNe explosions, two basic techniques i.e. broad-band polarimetry and spectropolarimetry have been used. Both of these techniques have advantages and disadvantages relative to each other. One of the main advantages of spectropolarimetry of SNe with respect to broad-band polarimetry is its ability to infer geometric and dynamical information for the different chemical constituents of the explosion. Broad-band polarimetric observations construct a rather rough picture of the stellar death but require lesser number of total photons than spectropolarimetry. Hence broad-band polarimetric observations can be extended to objects at higher red-shifts or/and they allow to enhance the polarimetric coverage and sampling of the light curve (LC), especially at epochs far from the maximum when the SN is dimmer.

The scope of this paper uses imaging polarimetric observations in *R*-band using a meter class telescope when the SN 2012aw was bright enough ($R < 13.20$ magnitude).

1.1 SN 2012aw

SN 2012aw was discovered in a face-on ($i \sim 54.6^\circ$, from HyperLEDA¹), barred and ringed spiral galaxy M95 (NGC 3351) by P. Fagotti on CCD images taken on 2012 March 16.85 UT with a 0.5-m reflector (cf. CBET 3054, Fagotti et al., 2012). The SN was located $60''$ west and $115''$ north of the center of the host galaxy with coordinates $\alpha = 10^h 43^m 53^s.73$, $\delta = +11^\circ 40' 17''.9$ (equinox 2000.0). This SN discovery was also confirmed independently by A. Dimai on 2012 March 16.84 UT, and J. Skvarc on March 17.90 UT (more information available in Fagotti et al. 2012, CBET 3054; see also special notice no. 269 available at AAVSO²). The spectra obtained on March 17.77 UT by Munari, Vagnozzi & Castellani (2012) with the Asiago Observatory 1.22-m reflector showed a very blue continuum, essentially featureless, with no absorption bands and no detectable emission lines. In subsequent spectra taken on March 19.85 UT (Itoh, Ui & Yamanaka, 2012) and 19.92 UT (Siviero et al., 2012), the line characteristics finally led to classify it as a young Type II-P supernova. The explosion date of this event is precisely determined by Fraser et al. (2012) and Bose et al. (2013).

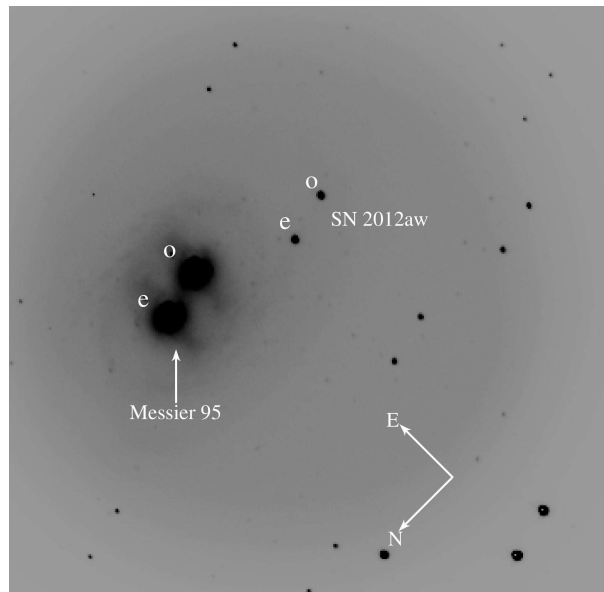


Figure 1. The *R*-band image of the SN 2012aw field around the host galaxy M95, observed on 17 April 2012 using AIMPOL with the 1-m ST, India. Each object has two images. The ordinary and extra-ordinary images of SN 2012aw and host galaxy are labeled as o and e, respectively. The galaxy is marked with a white arrow and the SN is located $60''$ west, $115''$ south of the center of M95 galaxy. North and East directions are also indicated.

We adopt 2012 March 16.1 ± 0.8 day (JD 2456002.6 \pm 0.8, taken from the later study) as time of explosion throughout this article. At a distance of about 10 Mpc (cf. Freedman et al., 2001; Russell, 2002; Bose et al., 2013), this event provided us a good opportunity to study its detail polarimetric properties.

The progenitor of this SN has been detected both in ground and space based pre-explosion images and its distinct characteristics are analyzed. In pre-SN explosion images obtained with *HST*³ + WFPC⁴, VLT⁵ + ISAAC⁶ and NTT⁷+SOFI⁸, Fraser et al. (2012) found that the progenitor is a red supergiant (mass 14–26 M_{\odot}). An independent study by Van Dyk et al. (2012) confirmed these findings (mass 15–20 M_{\odot}). However, Kochanek, Khan & Dai (2012) have a different view and have concluded that progenitor mass in earlier studies are significantly overestimated and that the progenitor’s mass is $< 15 M_{\odot}$. Immediately after the discovery, several groups have started the follow-up observations of this event in different wavelengths (see, e.g. Immler & Brown, 2012; Stockdale et al., 2012; Bayless et al., 2013; Munari et al., 2013; Yadav et al., 2013). Early epoch (4 to 270 days) low-resolution optical spectroscopic and dense photometric follow-up (in *UBVRI/griz* bands) observations of SN 2012aw has been analyzed by Bose et al. (2013). In a recent study, Jerkstrand et al. (2013), have presented nebular phase (between 250 – 451 days) optical and near-infrared spectra of this event and have analyzed it with spectral model calculations. Furthermore, the preliminary analysis of optical spectropolarimetric

³ Hubble Space Telescope

⁴ Wide-Field and Planetary Camera 2

⁵ Very Large Telescope

⁶ Infrared Spectrometer And Array Camera

⁷ New Technology Telescope

⁸ Infrared spectrograph and imaging camera

¹ <http://leda.univ-lyon1.fr> - Paturel et al. (2003)

² <http://www.aavso.org/aavso-special-notice-269>

Table 1. Polarimetric observation log and estimated polarimetric parameters of SN 2012aw.

UT Date (2012)	JD 2450000	Phase ^a (Days)	Observed		Intrinsic (ISP _{MW} subtracted)		Intrinsic (ISP _{MW} + ISP _{HG} subtracted)	
			$P_R \pm \sigma_{P_R}$ (%)	$\theta_R \pm \sigma_{\theta_R}$ (°)	$P_R \pm \sigma_{P_R}$ (%)	$\theta_R \pm \sigma_{\theta_R}$ (°)	$P_R \pm \sigma_{P_R}$ (%)	$\theta_R \pm \sigma_{\theta_R}$ (°)
Mar 26	6013.35	10.75	0.58 ± 0.46	131.4 ± 22.9	0.61 ± 0.46	138.9 ± 21.6	0.39 ± 0.46	134.2 ± 33.4
Mar 28	6015.23	12.63	0.56 ± 0.03	132.0 ± 1.5	0.60 ± 0.03	139.6 ± 1.4	0.38 ± 0.03	135.1 ± 2.2
Mar 29	6016.28	13.68	0.49 ± 0.08	132.2 ± 4.6	0.53 ± 0.08	140.8 ± 4.3	0.31 ± 0.08	136.1 ± 7.3
Apr 16	6034.18	31.58	0.24 ± 0.17	132.0 ± 21.0	0.30 ± 0.17	147.8 ± 16.7	0.07 ± 0.17	150.5 ± 72.8
Apr 17	6035.25	32.65	0.26 ± 0.01	142.6 ± 1.0	0.36 ± 0.01	154.0 ± 0.8	0.15 ± 0.01	164.8 ± 1.8
May 15	6063.05	60.45	0.87 ± 0.08	123.8 ± 2.6	0.85 ± 0.08	129.0 ± 2.6	0.68 ± 0.08	123.3 ± 3.3
May 19	6067.04	64.44	0.54 ± 0.01	124.3 ± 0.5	0.54 ± 0.01	132.7 ± 0.5	0.35 ± 0.01	123.6 ± 0.8
May 21	6069.08	66.48	0.43 ± 0.06	112.3 ± 4.0	0.37 ± 0.06	122.7 ± 4.6	0.28 ± 0.06	103.4 ± 6.2
Jun 14	6093.23	90.63	0.47 ± 0.14	128.2 ± 8.5	0.49 ± 0.14	137.5 ± 8.2	0.29 ± 0.14	129.9 ± 14.1

^a with reference to the explosion epoch JD 2456002.6

data of SN 2012aw, revealed that outer ejecta is substantially asymmetric (Leonard et al., 2012b).

In this paper, we present Cousins *R*-band polarimetric follow-up observations of SN 2012aw. The observations and data reduction procedures are presented in Section 2. Estimation of intrinsic polarization is described in Section 3. Finally, results and conclusions are presented in Sections 4 and 5, respectively.

2 OBSERVATIONS AND DATA REDUCTION

Polarimetric observations of SN 2012aw field were carried out during nine nights, i.e., 26, 28, 29 March; 16, 17 April; 15, 19, 21 May and 12 June 2012 using the ARIES Imaging Polarimeter (AIMPOL, Rautela et al., 2004) mounted at the Cassegrain focus of the 104-cm Sampurnanand telescope (ST) at Manora Peak, Nainital. This telescope is operated by the Aryabhata Research Institute of Observational sciences (ARIES), India. Complete log of these observations is presented in Table 1. The position of SN, which is fairly isolated from the host galaxy and lies on a smooth and faint galaxy background is shown in Fig. 1. The observations were carried out in *R* ($\lambda_{R_{eff}} = 0.67\mu\text{m}$) photometric band using liquid nitrogen cooled Tektronix 1024×1024 pixel² CCD camera. Each pixel of the CCD corresponds to 1.73 arcsec and the field-of-view (FOV) is ~ 8 arcmin in diameter on the sky. The full width at half-maximum of the stellar images vary from 2 to 3 pixel. The readout noise and the gain of the CCD are $7.0 e^-$ and $11.98 e^-/\text{ADU}$ respectively.

The AIMPOL consists of a half-wave plate modulator and a Wollaston prism beam-splitter. In order to obtain the measurements with good signal-to-noise ratio, images that were acquired at each position of half-wave plate were combined. Since AIMPOL is not equipped with a narrow-window mask, care was taken to exclude the stars that have contamination from the overlap of ordinary and extraordinary images of one star on the same of another star in the FOV.

Fluxes of ordinary (I_o) and extra-ordinary (I_e) beams of the SN and field stars with good signal-to-noise ratio were extracted by standard aperture photometry after preprocessing using the IRAF⁹ package. The ratio $R(\alpha)$ is given by:

$$R(\alpha) = \frac{\frac{I_e(\alpha)}{I_o(\alpha)} - 1}{\frac{I_e(\alpha)}{I_o(\alpha)} + 1} = P \cos(2\theta - 4\alpha), \quad (1)$$

Where, P is the fraction of the total linearly polarized light and, θ is the polarization angle of the plane of polarization. Here α is the position of the fast axis of the half-wave plate at 0° , 22.5° , 45° and 67.5° corresponding to the four normalized Stokes parameters respectively, q [$R(0^\circ)$], u [$R(22.5^\circ)$], q_1 [$R(45^\circ)$] and u_1 [$R(67.5^\circ)$]. The detailed procedures used to estimate the polarization and polarization angles for the programme stars are described by Ramaprakash et al. (1998); Rautela et al. (2004) and Medhi et al. (2010). Since polarization accuracy is, in principle, limited by photon statistics, we estimated the errors in normalized Stokes parameters $\sigma_{R(\alpha)}$ (σ_q , σ_u , σ_{q_1} and σ_{u_1} in %) using the expression (Ramaprakash et al., 1998):

$$\sigma_{R(\alpha)} = \sqrt{(N_e + N_o + 2N_b)/(N_e + N_o)} \quad (2)$$

Where, N_e and N_o are the counts in extra-ordinary and ordinary rays respectively, and $N_b [= \frac{N_{be} + N_{bo}}{2}]$ is the average background counts around the extra-ordinary and ordinary rays of a source. The individual errors associated with the four values of $R(\alpha)$, estimated using equation (2), are used as weights in the calculation of P and θ for the programme stars.

To correct the measurements for the instrumental polarization and the zero-point polarization angle, we observed a number of unpolarized and polarized standards, respectively, taken from Schmidt et al. (1992). Measurements for the standard stars are compared with those taken from the Schmidt et al. (1992). The observed values of degree of polarization ($P(\%)$) and position angle ($\theta(^\circ)$) were in good agreement (within the observational errors) with those published in Schmidt et al. (1992). The instrumental polarization of AIMPOL on the 1.04-m ST has been characterized and monitored since 2004 for different projects and found to be $\sim 0.1\%$ in different bands (e.g., Rautela et al., 2004; Pandey et al., 2009; Eswaraiyah et al., 2011, 2012, 2013, and references therein).

3 ESTIMATION OF INTRINSIC POLARIZATION

The observed polarization measurements of a distant SN could be composed of various components such as interstellar polarization due to Milky Way dust (ISP_{MW}), interstellar polarization due to host galactic dust (ISP_{HG}) and due to instrumental polarization. As described in the previous section, we have already subtracted the instrumental polarization. Therefore, now it is essential to estimate

⁹ IRAF is the Image Reduction and Analysis Facility distributed by the National Optical Astronomy Observatories, which are operated by the Association of Universities for Research in Astronomy, Inc., under cooperative agreement with the National Science Foundation.

Table 2. Observational detail of 14 isolated field stars selected to subtract the interstellar polarization. Observations of all field stars were performed on 20 January 2013 in *R* band with the 1.04 m ST. All these stars were selected with known distances and within 10° radius around SN 2012aw. The distance mentioned in the last column has been taken from van Leeuwen (2007) catalogue.

Star id	RA (J2000) ($^\circ$)	Dec (J2000) ($^\circ$)	$P_R \pm \sigma_{P_R}$ %	$\theta_R \pm \sigma_{\theta_R}$ ($^\circ$)	Distance (in pc)
HD 99028 [†]	170.98071	+10.52960	0.08 ± 0.00	167.9 ± 1.7	23.7 ± 0.5
HD 88830 [†]	153.73935	+09.21180	0.10 ± 0.01	116.8 ± 1.8	36.3 ± 3.8
HD 87739 [†]	151.78235	+08.76970	0.05 ± 0.01	99.9 ± 6.6	85.0 ± 8.3
HD 97907 [†]	168.96624	+13.30750	0.17 ± 0.05	59.6 ± 9.5	99.6 ± 12.1
HD 88282 [†]	152.72730	+07.69460	0.12 ± 0.01	79.1 ± 1.8	118.5 ± 10.0
HD 87635 [†]	151.57707	+07.94470	0.17 ± 0.00	89.0 ± 0.5	135.7 ± 19.9
HD 87915 [†]	152.08824	+07.57300	0.11 ± 0.01	86.4 ± 1.6	193.1 ± 34.7
HD 87996 [†]	152.20123	+06.71740	0.20 ± 0.04	62.5 ± 5.6	243.3 ± 91.2
HD 88514 [†]	153.15102	+07.67730	0.18 ± 0.03	90.5 ± 4.5	254.5 ± 82.9
G 452	160.45186	+12.10886	0.10 ± 0.01	22.6 ± 2.4	261.1 ± 70.9
BD+12 2250	161.08996	+11.33560	0.12 ± 0.08	100.1 ± 18.0	286.5 ± 91.1
BD+13 2299	161.41026	+12.46724	0.20 ± 0.00	72.4 ± 0.8	314.5 ± 87.0
HD 93329	161.65268	+11.18412	0.12 ± 0.03	144.8 ± 5.8	358.4 ± 118.2
HD 92457	160.15550	+12.07868	0.05 ± 0.07	27.8 ± 41.3	460.8 ± 191.1

[†] Stars with available *V*-band polarimetry from Heiles (2000) catalogue.

BD+12 2250, BD+13 229, G 452, HD 93329 and HD 92457 are the stars within 2° radius field around the SN.

the contributions due to ISP_{MW} and ISP_{HG} , and to remove them from the total observed polarization measurements of SN. However, there is no totally reliable method to derive the ISP_{MW}/ISP_{HG} of SN polarimetry observationally and utmost careful analysis is required to avoid any possible fictitious result. In the following sections, we discuss in detail about the ISP_{MW} and ISP_{HG} estimation in the present set of observations.

3.1 Interstellar polarization due to Milky Way (ISP_{MW})

To estimate the interstellar polarization in the direction of SN 2012aw, we have performed *R*-band polarimetric observations of 14 isolated and non-variable field stars (which do not show either emission features or variability flag in the SIMBAD database) distributed in a region of 10° radius around SN. All 14 stars have distance information from Hipparcos parallax (van Leeuwen, 2007) and out of these, 9 stars have both polarization (Heiles, 2000) and distance measurements. In Fig. 2 (left panels), we show the distribution of degree of polarization and polarization angles for these 9 stars. The weighted mean values of P_V and θ_V of 8 out of these 9 stars (after excluding one star whose P_V is 0.007%) are found to be $0.071\% \pm 0.010\%$ and $83^\circ \pm 4^\circ$, respectively. Because our polarimetric observations are performed in the *R*-band therefore, to correct for ISP_{MW} component and to study the intrinsic behavior of SN, we have used polarization measurements of 14 field stars observed on 20 January 2013 in *R*-band. The distribution of P_R and θ_R values of these stars is shown in right panels of Fig. 2. All the observed 14 stars are shown with filled circles. As revealed by both left and upper right panels of Fig. 2, the amount of degree of polarization shows an increasing trend with distance. It is worthwhile to note that, in the upper right panel, the degree of polarization (P_R) seems to show a sudden jump from $\sim 0.1\%$ at the distance of ~ 100 pc to $\sim 0.2\%$ at a distance of ~ 250 pc, thereby indicating the presence of a dust layer (shown with a gray region in Fig. 2) at ~ 100 pc. Whereas, the polarization angles of the stars from Heiles catalogue (left bottom panel) and those observed from the present set-up in *R*-band (except few stars) are distributed between $50^\circ - 100^\circ$ as shown with the dashed lines (in Fig. 2). The Gaussian mean value

of θ_R using 14 stars is found to be $\sim 82^\circ$. This indicates the presence of a uniform dust layer towards the direction of SN2012AW, which nearly contributes $\sim 0.1\%$ to $\sim 0.2\%$ of polarization and having a mean magnetic field orientation $\sim 82^\circ$. Therefore, we believe that most probably, the ISP_{MW} component has been dominated by the contribution from this dust layer.

To determine the ISP_{MW} component, firstly the P_R and θ_R values of all field stars as well as SN were transformed into Stokes parameters using the following relations¹⁰:

$$Q_R = P_R \cos 2\theta_R \quad (3)$$

$$U_R = P_R \sin 2\theta_R \quad (4)$$

Then, the weighted mean Stokes parameters were estimated by considering (a) all 14 field stars distributed over all distances, and (b) only 10 field stars distributed beyond the distance of 100 pc. These weighted Stokes parameters ($\langle U_R \rangle$, $\langle Q_R \rangle$) were converted back to P_R and θ_R using the following relations:

$$P_R = \sqrt{Q_R^2 + U_R^2} \quad (5)$$

$$\theta_R = 0.5 \times \arctan\left(\frac{U_R}{Q_R}\right) \quad (6)$$

The $\langle U_R \rangle$, $\langle Q_R \rangle$, $\langle P_R \rangle$ and $\langle \theta_R \rangle$ values (as estimated by two ways) are listed in Table 3. It is clear from this table that the $\langle P_R \rangle$ of 14 stars is relatively smaller than that determined using 10 stars. This could be due to the fact that the weighted mean values for stars at all distances may skew the result towards the brighter and more nearby stars which likely to be incorrect. Whereas the $\langle \theta_R \rangle$ values in two cases nearly matches with each other and mimic the mean magnetic field orientation ($\sim 82^\circ$) of the dust layer as noticed above. To avoid the values biased towards lower end due to nearby and brighter stars, we have considered the polarization measurements of 10 stars distributed beyond 100 pc distance to

¹⁰ Our polarimeter and software have been designed in such a way that we get P and θ through fitting the equation 1 on four Stokes parameters obtained at four positions of half-wave plate as mentioned in Section 2

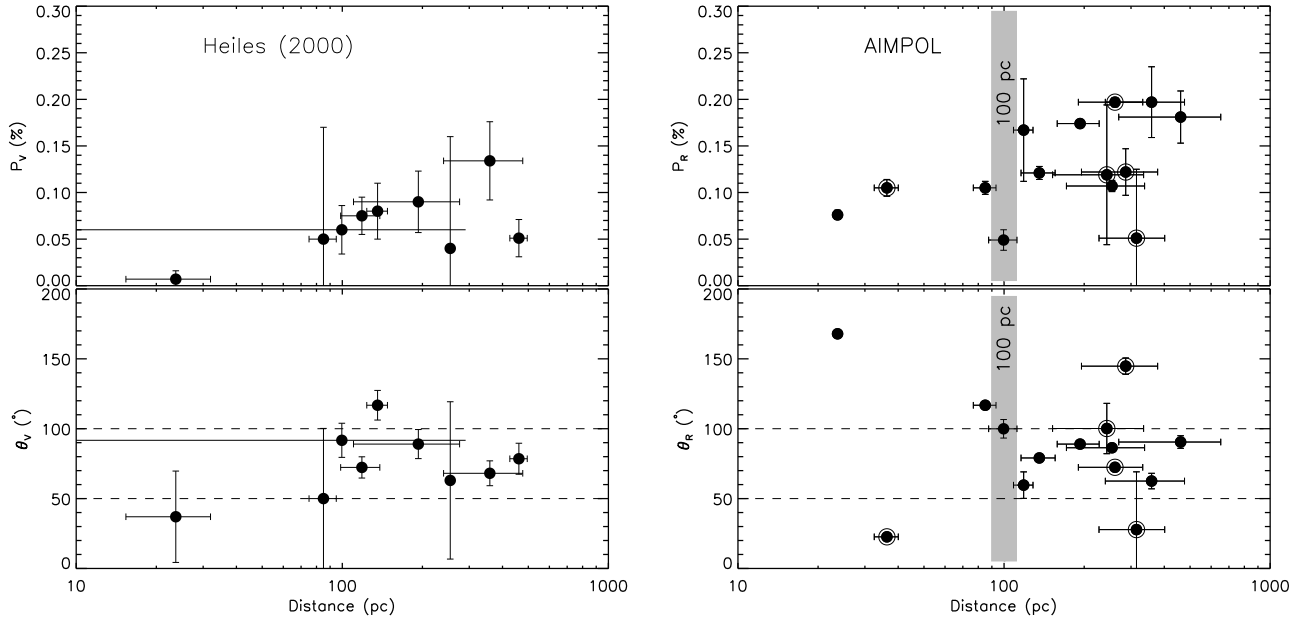


Figure 2. Distribution of polarization and polarization angle of stars around SN 2012aw. Left panel: 9 isolated field stars with known polarization and parallax measurements from Heiles (2000) and van Leeuwen (2007), respectively. Right panel: same as left panel but for 14 isolated stars with R band polarimetric data using AIMPOL and with distance from van Leeuwen (2007) catalogue. Filled circles denote 9 common stars in both left and right panels. The encircled filled circles are 5 stars distributed within a 2° radius around the location of SN 2012aw. The gray region represents the possible presence of a dust layer around 100 pc distance.

Table 3. Estimated polarimetric parameters for ISP_{MW} (see Section 3.1 for detail).

Number of stars	Distance (pc)	$\langle Q_R \pm \sigma_{Q_R} \rangle$ (%)	$\langle U_R \pm \sigma_{U_R} \rangle$ (%)	$\langle P_R \pm \sigma_{P_R} \rangle$ (%)	$\langle \theta_R \pm \sigma_{\theta_R} \rangle$ ($^\circ$)
14 [#]	all distances	-0.101 ± 0.002	0.012 ± 0.002	0.102 ± 0.002	86.49 ± 0.54
10	> 100	-0.154 ± 0.002	0.032 ± 0.002	0.157 ± 0.002	84.10 ± 0.43

[#] All stars within 10° radius around the SN.

estimate the ISP_{MW} component. In addition, using these 10 stars which are distributed beyond 100 pc essentially may take care of the contribution from the dust layer at the distance of 100 pc. Therefore, we consider $\langle Q_R \rangle = -0.154 \pm 0.002\%$, $\langle U_R \rangle = 0.032 \pm 0.002\%$ values as the ISP_{MW} component (i.e. $\langle Q_{ISP_{MW}} \rangle = \langle Q_R \rangle$ and $\langle U_{ISP_{MW}} \rangle = \langle U_R \rangle$). These weighted mean values have been subtracted vectorially from the Stokes parameters of the SN using the relations:

$$Q_{int} = Q_{SN} - \langle Q_{ISP_{MW}} \rangle \quad (7)$$

$$U_{int} = U_{SN} - \langle U_{ISP_{MW}} \rangle \quad (8)$$

Where Q_{SN} , U_{SN} and Q_{int} , U_{int} denote respectively the observed and intrinsic (ISP_{MW} corrected) Stokes parameters of the SN. The resultant intrinsic Stokes parameters (Q_{int} , U_{int}) were converted into P_{int} and θ_{int} using the relations 5 and 6. These intrinsic values of SN are respectively listed in column 6 and 7 in Table 1 and plotted in Fig. 4(a) and (b), with filled circles connected with a thick line.

The reddening, $E(B - V)$ due to Milky Way dust in the direction of SN 2012aw, as derived from the 100- μ m all-sky dust extinction map of Schlegel, Finkbeiner & Davis (1998), was found to be 0.0278 ± 0.0002 mag. According to the mean polariza-

tion efficiency relation $P_{mean} = 5 \times E(B - V)$ (Serkowski et al., 1975), the polarization value is estimated to be $P_{mean} \sim 0.14\%$ which closely matches with the weighted mean polarization value, $0.157 \pm 0.002\%$ obtained using the 10 fields stars distributed beyond 100 pc distance (cf. Table 3). It is clear that polarization values obtained both from the present observations of the field stars and mean polarization efficiency relation are similar which implies that the dust grains in the local interstellar medium (ISM) exhibit mean polarization efficiency.

3.2 Interstellar polarization due to host galactic dust (ISP_{HG})

The reddening, $E(B - V)$, due to dust in the SN 2012aw host galaxy was found to be 0.046 ± 0.008 mag (see Bose et al., 2013). This value was derived using the empirical correlation, between reddening and Na I D lines, given by Poznanski et al. (2012). As described in Section 3.1, the weighted mean value of polarization of 10 field stars situated beyond 100 pc distance ($0.157\% \pm 0.002\%$) and the extinction (0.0278 ± 0.0002 mag) due to the Galactic dust in the line of sight to the SN suggest that Galactic dust exhibits a mean polarization efficiency. To subtract the ISP_{HG} component we should estimate the degree of polarization and the magnetic field orientation of the host galaxy at the location of the SN.

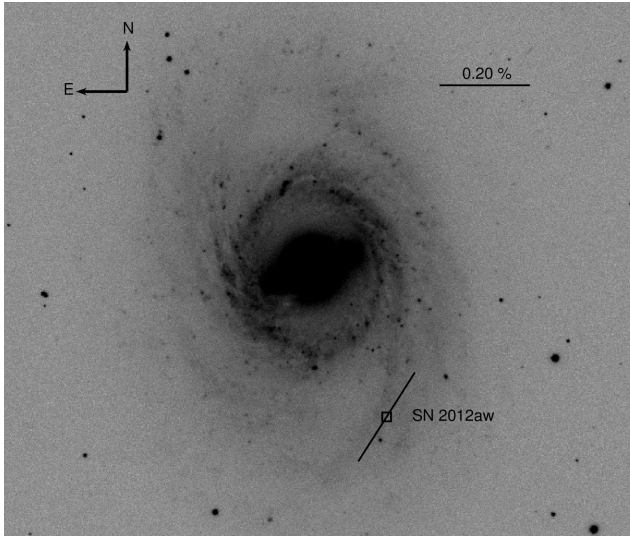


Figure 3. SDSS g -band image (7.7×7.2) of the SN field containing the galaxy M95. A vector with a degree of polarization 0.23% and position angle of 147° is drawn at the location of SN 2012aw (see text in Section 3.2 for details). A vector with a 0.20% polarization and polarization angle of 90° is shown for a reference (top right). The approximate orientation of the magnetic field at the location of SN has been determined on the basis of structure of the spiral arm (see Section 3.2 for more details). The location of the SN is represented by a square symbol. North is up and east is left as shown in the figure.

The properties of dust grains in the nearby galaxies have been investigated in detail only in a handful of cases and diverse nature of dust grains have been established in these studies. In case of SN 1986G, Hough et al. (1987) probed the ISP_{HG} component due to the dust lanes in the host galaxy NGC 5128 (Centaurus A) and validated that the size of the dust grains is smaller than typical Galactic dust grains. In another study (SN 2001el), the grains size were found to be smaller for NGC 1448 (Wang et al., 2003a). However, in some cases polarization efficiency of dust has been estimated to be much higher than the typical Galactic dust (see e.g. Leonard et al., 2002; Clayton et al., 2004). For the present study, we assume that the dust grain properties of the M95 are similar to that the Galactic dust, and follow mean polarization efficiency relation (i.e. $P_{mean} = 5 \times E(B - V)$; Serkowski et al. 1975). Therefore, the estimated polarization value would be $\sim 0.23\%$.

Another required parameter is the orientation of the magnetic field near the location of the SN. It is well known that large-scale Galactic magnetic field runs almost parallel (i.e. perpendicular to the line connecting a point with the galaxy center) to the spiral arms (Scarrott et al., 1990, 1991; Heiles, 1996; Han, 2009). Interestingly, as shown in Fig. 1, the SN 2012aw is located nearer to one of the spiral arms of the host galaxy. On the basis of the structure of the spiral arm and the location of SN, we have estimated the tangent to the spiral arm at the location of the SN (see Fig. 3), which makes approximately 147° from the equatorial north increasing towards the east. We assume, on the basis of structure of the spiral arms and the magnetic field orientation that the magnetic field orientation in the host galaxy at the location of the SN is to be $\sim 147^\circ$. Here, we would like to emphasize that present procedure of considering magnetic field for the host of SN 2012aw is well established in previous spectropolarimetric studies of Type IIP SN 1999em (Leonard et al., 2001) and Type IIb SN 2001ig (Maund et al., 2007).

As shown in the Fig. 3, a black vector with a length of 0.23%

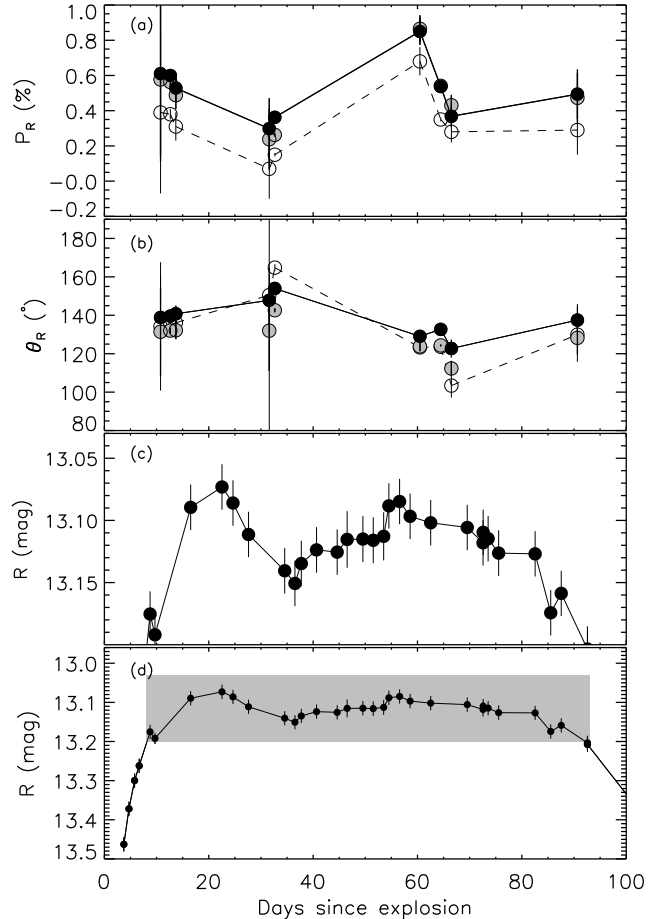


Figure 4. Panels (a) and (b): Temporal evolution of polarization and polarization angles of SN 2012aw in R band, respectively. Filled circles connected with thick lines denote the temporal evolution of polarization and polarization angles after subtracting the ISP_{MW} component only, whereas those corrected for both $ISP_{MW} + ISP_{HG}$ components were represented with open circles connected with broken lines. The observed polarization parameters are shown with gray filled circles in panels (a) and (b). The bottom panel (d) shows the calibrated R band LC of SN 2012aw obtained with ST (see Bose et al., 2013). The photometric data shown with shaded region in the bottom panel (d) is re-plotted in panel (c) for a better clarity.

and orientation of 147° is drawn at the location of the SN which is shown with a square symbol. Hence, by assuming that the amount of polarization and the polarization angle due to the host galaxy are as 0.23% and 147° , the Stokes parameters are estimated to be $Q_{ISP_{HG}} = 0.11\%$, $U_{ISP_{HG}} = -0.25\%$. To get the intrinsic Stokes parameters and hence the amount of polarization and polarization angles purely due to the SN 2012aw, these values were subtracted vectorially from the ISP_{MW} corrected Stokes parameters as described in Section 3.1. The intrinsic ($ISP_{MW} + ISP_{HG}$ subtracted) polarization and polarization angles of SN are listed in the Columns 8 and 9 of Table 1 and plotted in the Fig. 4 (a) and (b), respectively, with open circles connected with broken lines.

Table 4. Observed and intrinsic (ISP_{MW} and ISP_{MW} + ISP_{HG} subtracted) $Q - U$ parameters for SN 2012aw.

UT Date (2012)	JD 2450000	Phase ^a (Days)	Observed		Intrinsic (ISP _{MW} subtracted)		Intrinsic (ISP _{MW} + ISP _{HG} subtracted)	
			$Q_R \pm \sigma_{Q_R}$ (%)	$U_R \pm \sigma_{U_R}$ (%)	$Q_R \pm \sigma_{Q_R}$ (%)	$U_R \pm \sigma_{U_R}$ (%)	$Q_R \pm \sigma_{Q_R}$ (%)	$U_R \pm \sigma_{U_R}$ (%)
Mar 26	6013.35	10.75	-0.072 ± 0.461	-0.573 ± 0.464	0.082 ± 0.461	-0.605 ± 0.464	-0.012 ± 0.461	-0.394 ± 0.464
Mar 28	6015.23	12.63	-0.058 ± 0.029	-0.560 ± 0.029	0.095 ± 0.029	-0.592 ± 0.029	0.002 ± 0.029	-0.382 ± 0.029
Mar 29	6016.28	13.68	-0.048 ± 0.079	-0.486 ± 0.078	0.106 ± 0.079	-0.518 ± 0.078	0.012 ± 0.079	-0.308 ± 0.078
Apr 16	6034.18	31.58	-0.025 ± 0.174	-0.237 ± 0.173	0.129 ± 0.174	-0.269 ± 0.173	0.035 ± 0.174	-0.059 ± 0.173
Apr 17	6035.25	32.65	0.069 ± 0.010	-0.254 ± 0.009	0.223 ± 0.010	-0.286 ± 0.009	0.129 ± 0.010	-0.076 ± 0.009
May 15	6063.05	60.45	-0.330 ± 0.077	-0.800 ± 0.077	-0.176 ± 0.077	-0.832 ± 0.077	-0.269 ± 0.077	-0.622 ± 0.077
May 19	6067.04	64.44	-0.198 ± 0.009	-0.504 ± 0.009	-0.044 ± 0.010	-0.536 ± 0.009	-0.137 ± 0.010	-0.326 ± 0.009
May 21	6069.08	66.48	-0.307 ± 0.059	-0.303 ± 0.059	-0.153 ± 0.059	-0.335 ± 0.059	-0.247 ± 0.059	-0.125 ± 0.059
Jun 14	6093.23	90.63	-0.111 ± 0.141	-0.460 ± 0.140	0.043 ± 0.141	-0.492 ± 0.140	-0.050 ± 0.141	-0.282 ± 0.140

^a with reference to the explosion epoch JD 2456002.6

4 DISCUSSION

4.1 Polarization light curve (PLC) analysis

In this section, we analyze the evolution of the PLC and its possible resemblance with the photometric light curve (LC) of the SN 2012aw as shown in Fig 4. The calibrated R -band magnitudes have been taken from Bose et al. (2013) which shows different evolutionary phases of the LC as described in Grassberg et al. (1971); Falk & Arnett (1977); Utrobin (2007). Since in the present study, polarimetric data sets are limited upto the plateau phase, in Fig. 4 (panels c and d), only the adiabatic cooling phase and the phase of cooling and recombination wave are shown.

The temporal variation of ISP_{MW} corrected degree of polarization (P_R) values (shown with filled circles, Fig. 4a) shows a maximum and minimum values of $\sim 0.9\%$ and $\sim 0.3\%$, respectively with a possible trend of variations in accordance with the R -band LC as shown in the panel 4(c). Although there is a significant reduction in ISP_{MW} + ISP_{HG} corrected P_R values (open circles, Fig. 4a), its resemblance with photometric light curve (panel c) remain similar. However, both ISP_{MW} and ISP_{MW} + ISP_{HG} corrected polarization angles (θ_R , shown with filled circles in Fig. 4(b)) does not show much variation during the similar epochs of observations and are distributed around a weighted mean value of $\sim 138^\circ$. Interestingly, first (10–14 days) three measurements of ISP_{MW} corrected P_R and θ_R are almost constant. During this adiabatic cooling phase, the SN LC seems to be brightened by ~ 0.12 magnitude as shown in the Fig. 4c.

It is worthwhile to note that dips observed around 35 days in the LC of the SN and in the ISP_{MW} + ISP_{HG} corrected P_R are temporally correlated with a minimum amount of polarization ($\sim 0.07\%$). This observed feature during the end of the adiabatic cooling or early recombination phase could be attributed to several reasons e.g., (i) changes in the geometry i.e., transition from more asphericity to sphericity of SN, (ii) modification in density of scatterers (electrons and/or ions), (iii) mechanism of scattering i.e., single and (or) multiple scattering, (iv) changes in the clumpiness in the SN envelope, (v) changes in the electron-scattering atmosphere of SN, and (vi) interaction of SN with a dense circumstellar medium. In the recombination phase (~ 40 days onwards), the evolution in the values of ISP_{MW} + ISP_{HG} corrected P_R and θ_R are in such a way that the amount of polarization shows an increasing trend. This increasing trend could suggest that during the recombination phase and onwards, the geometry of the SN envelope could have acquired more asphericity

If we assume that the ISP_{MW} and ISP_{HG} components are con-

stant, then the changes observed in the temporal variation of intrinsic polarization measurements of the SN could purely be attributed to variations in the geometry of the SN along with the other possible reasons such as the interaction of the SN shock with the ambient medium. However, these properties could be well addressed using high resolution spectroscopic/spectropolarimetric investigations which are beyond the scope of this paper.

4.2 Q and U parameters

The $Q - U$ parameters, representing different projections of the polarization vectors, are used as a powerful tool to examine the simultaneous behavior of the polarization and the polarization angle with wavelengths (see e.g. Wang et al., 2003a,b). The pattern of the variation in $Q - U$ plane does not depend upon the ISP_{MW}/ISP_{HG} corrections. However, the ISP_{MW}/ISP_{HG} subtracted parameters are dependent on the corrections applied to the observed values. A small change in ISP_{MW}/ISP_{HG} may considerably affect the polarization angle (PA) values.

The estimated $Q - U$ parameters (observed and intrinsic) for SN 2012aw are presented in Table 4 and are plotted in Fig. 5. The left and middle panels of this figure show the observed and ISP_{MW} subtracted parameters and, the right panel represents intrinsic parameters after subtracting both ISP_{MW} + ISP_{HG} contribution as discussed in Section 3. The square symbol connected with large circles drawn nearer to the solar neighborhood in the middle and right panels respectively indicate ISP_{MW} ($Q_{ISP_{MW}} = -0.154$, $U_{ISP_{MW}} = 0.032$) and ISP_{MW} + ISP_{HG} ($Q_{ISP_{MW}+ISP_{HG}} = -0.060$, $U_{ISP_{MW}+ISP_{HG}} = -0.178$) components.

Since, in the present case, the data points are limited, a firm conclusion could not be robustly drawn on behalf of Q and U parameters. However, it seems that in all three panels of Fig. 5, these data points show scattered distribution, which seems to form a loop like structure on $Q - U$ plane. This kind of structure has been also observed in case of SN 1987A (Cropper et al., 1988), SN 2004dj (Leonard et al., 2006) and SN 2005af (Pereyra et al., 2006). Although, it is to be noted that if we ignore one of the data points (observed on 21 May), the variation of $Q - U$ parameters will more likely to follow straight line and in this case the previous interpretation may not be true.

4.3 Comparison with other Type IIP events

We have collected polarization parameters of a few well-observed Type IIP SNe from literature: SN 2008bk (Leonard et al., 2012a),

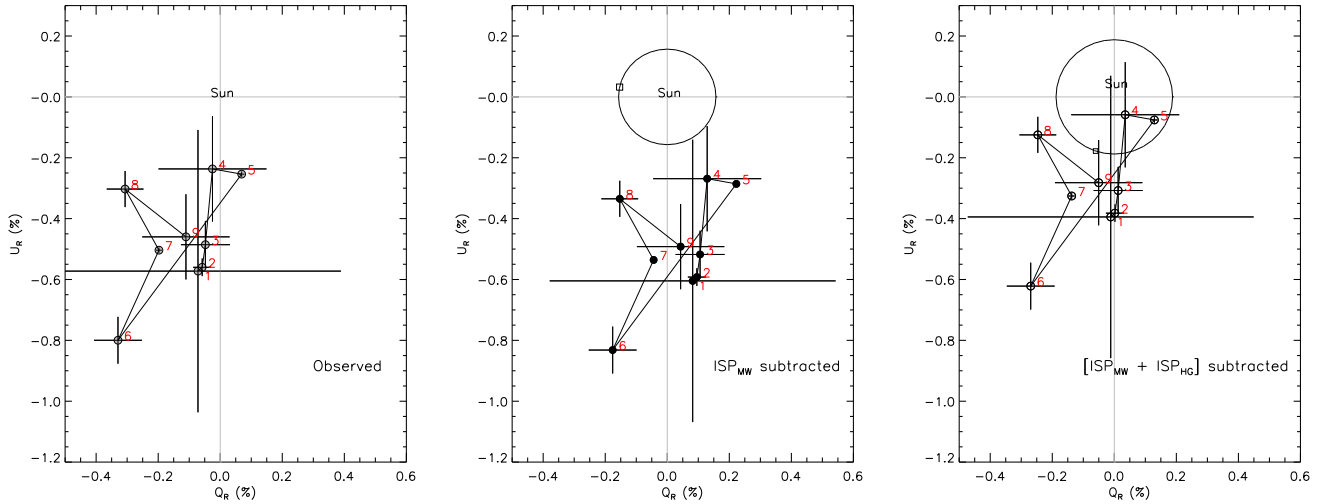


Figure 5. Stokes Q and U parameters of SN 2012aw. Left panel: Gray filled circles are the observed parameters. Middle panel: The data have been corrected for the ISP_{MW} component only (black filled circle; see text). Right panel: After correcting both $ISP_{MW} + ISP_{HG}$ components (open circle; see text). The square symbol connected with large circles drawn nearer to the solar neighborhood in the middle and right panels, respectively, indicate the ISP_{MW} and $ISP_{MW} + ISP_{HG}$ components. Numbers labelled with 1 to 9 (red colour) and connected with continuous lines, indicate the temporal order.

SN 2007aa and SN 2006ov (Chornock et al., 2010), 2005af (Pereyra et al., 2006) 2004dj (Leonard et al., 2006), 1999em (Leonard et al., 2001) and SN 1987A (Barrett, 1988) for which polarimetric observations have been performed for two or more epochs. Except for SN 1987A, SN 2005af and SN 2012aw, the data for other events are spectropolarimetric only. The intrinsic polarization values of SN 2012aw along with other SNe are plotted in Fig. 6. It is worthwhile to note that the explosion epochs of SN 1987A (see Hirata et al., 1987; Bionta et al., 1987), SN 1999em (see Elmhamdi et al., 2003) and SN 2012aw are known precisely, but there is uncertainty in the estimation of explosion epoch for other events (SN 2004dj, SN 2005af, SN 2006ov, SN 2007aa and SN 2008bk). In case of SN 2004dj, Leonard et al. (2006) considered the explosion epoch on JD 2453200.5 but Zhang et al. (2006) estimated it on JD 2453167 \pm 21. With an uncertainty of few weeks, the explosion epoch for SN 2005af is estimated to be on JD 2453379.5 (see Kotak et al., 2006). For SN 2006ov, Blondin et al. (2006) estimated the expected date of explosion \sim 36 days before the discovery (Nakano et al., 2006) but Li et al. (2007) reasonably constraints its explosion about 3 months before the discovery. We follow the later study in the present analysis. Similarly we considered explosion epoch for SN 2007aa, \sim 20 days before the discovery (see Doi et al., 2007; Folatelli et al., 2007) and for SN 2008bk, JD 2454550 (2008 March 24) has been considered as explosion epoch (see Morrell & Stritzinger, 2008; Van Dyk et al., 2010).

Shifting the phase (days after the explosion) by 21 days, the evolution of degree of polarization of SN 2004dj is very much similar to what has been seen in case of SN 2012aw as shown in the Fig. 6. However, it is important to mention that in case of SN 2004dj the degree of polarization increases after the end of the plateau phase (when we see through the H-rich shell); whereas for SN 2012aw, the degree of polarization increases (around 60 days) during the plateau phase which could be a possible indication of a diverse nature of the two events. However, it is noticeable that like SN 2008bk, SN 2012aw is also strongly polarized well before the end of the plateau (see Leonard et al., 2012a), indicating a possible

similarity in the both events. In the early phase (\sim 10 – 30 days), the ISP_{MW} corrected PLC of SN 2012aw matches with that of the SN 1987A, whereas in the later phase (\sim 30 – 45 days) it is closely matching with that of SN 2005af. Nonetheless, it is worthwhile to mention that to derive the polarization parameters of SN 1987A and SN 2005af, the ISP_{HG} components are not subtracted in respective studies. The polarimetric observations of SN 1999em are sparse; the polarization levels at different epochs seems to match with the $ISP_{MW} + ISP_{HG}$ corrected PLC of SN 2012aw. It is also obvious from figure 6 that the polarization values of SN 2006ov remains more than 1% for all three epoch observations which is higher than that of any of the Type IIP events in the list. Fig. 6 gives an important information regarding the evolution of ejecta of similar types of SNe. By comparing the PLCs of various IIP SNe shown with different symbols in Fig. 6 (filled star: SN 1987A, filled triangle: SN 1999em, filled square: SN 2004dj, open star: SN 2005af, open triangle: SN 2006ov, cross: SN 2007aa, open square: SN 2008bk and for SN 2012aw symbols are the same as in Fig. 4), it could be conjectured that the properties of the ejecta from Type IIP SNe are diverse in nature as noticed by Chornock et al. (2010).

We have also compared the ISP_{MW} and ISP_{HG} corrected PLCs of SN 2012aw with those of other Type Ib/c CCSNe. Type Ib/c SNe are naturally more asymmetric in comparison to that of Type IIP SNe because they lack a thick He blanket that smear out the internal geometry. Therefore, a higher degree of polarization is observed in case of Type Ib/c SNe. In the present analysis, PLC of SN 2012aw is also clearly showing a lower degree of polarization in comparison to well studied various Type Ib/c CCSNe (e.g. SN 2007uy, SN 2008D; Gorosabel et al., 2010). However, it is important to note that the P_R peak value for SN 2012aw seen at \sim 60 days is slightly less than the intrinsic polarization value of \sim 1% for the Type Ic SN 2008D which was related to violent X-ray transient (see Gorosabel et al., 2010). Here it is noticeable that present PLC interpretations of SN 2012aw depend a lot on a single data point (May 15) which is significantly higher in the percentage polarization than the data taken at other epochs.

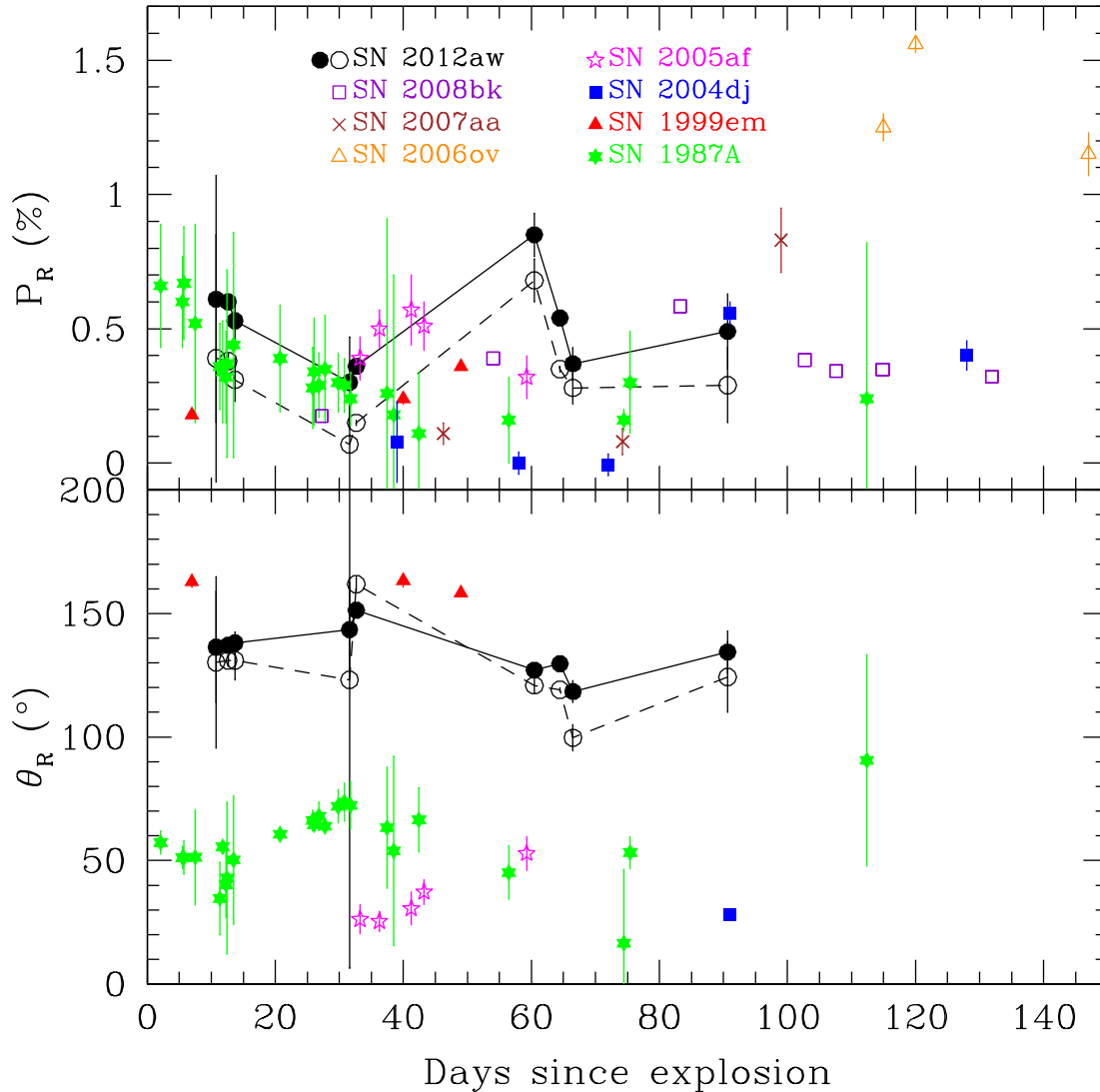


Figure 6. Comparison of polarization and polarization angle values of SN 2012aw with those of other Type IIP SNe: SN 1987A, SN 1999em, SN 2004dj, SN 2005af, SN 2006ov, SN 2007aa and SN 2008bk. The upper and lower panels show the degree of polarization and polarization angle, respectively. All values are intrinsic to a particular SN and symbols used in both panels are same. Thick and broken lines denote ISP_{MW} and both $ISP_{MW} + ISP_{HG}$ subtracted components, respectively for SN 2012aw.

5 CONCLUSIONS

We present results based on 9 epoch R band imaging polarimetric observations of Type IIP supernova SN 2012aw. To the best of our knowledge, the initial three epoch polarimetric observations presented here are the earliest optical polarimetric data reported for this event. It was not possible to monitor the SN during the beginning of the nebular or post-nebular phase due to observational constraints, however present observations cover almost up to the end of the plateau phase (~ 90 days). The main results of our present study are the following:

- The observed broad-band polarization for initial three epochs is $\sim 0.6\%$, then decreases up to $\sim 0.3\%$ following a sudden increase up to $\sim 0.9\%$ on 15 May 2013 and at later epochs it seems to show a declining trend. However, the observed polarization angle is almost constant, superimposed with slight variations.

- To study the intrinsic polarization properties of SN 2012aw, we subtracted the contribution due to ISP_{MW} and ISP_{HG} from the observed P and θ values of SN. The ISP_{MW} component was determined using the polarimetric observations of 10 field stars distributed within 10° radius around SN and located beyond 100 pc distance. The estimated Stokes parameters of ISP_{MW} are found to be $\langle Q_{ISP_{MW}} \rangle = -0.154 \pm 0.002\%$ and $\langle U_{ISP_{MW}} \rangle = 0.032 \pm 0.002\%$ (equivalent to $\langle P_{ISP_{MW}} \rangle = 0.157 \pm 0.002$ and $\langle \theta_{ISP_{MW}} \rangle = 84.10^\circ \pm 0.56^\circ$). We also estimated the degree of polarization (0.23%) and polarization angle (147°) at the location of SN by using the extinction value from Schlegel map assuming that the host galactic dust follow the mean polarization efficiency and the magnetic field in the host galaxy follow the structure of the spiral arms.

- The intrinsic polarization parameters of SN 2012aw follow trends of the photometric LC which could be attributed to the small scale variations in the SN atmosphere or their interaction with the ambient medium.

• Polarimetric parameters of this SN are compared with other well studied Type IIP events. During the early phase ($\sim 10 - 30$ days), the ISP_{MW} subtracted PLC of SN 2012aw matches with that of SN 1987A whereas at later epochs ($\sim 30 - 45$ days) it matches to that of SN 2005af.

ACKNOWLEDGMENTS

We are grateful to the observers Archana Soam, Manoj Kumar Patel and Ram Kesh Yadav at the Aryabhata Research Institute of observational sciences (ARIES) for their valuable time and support for the observations of this event. SBP and BK acknowledge the support of the Indo-Russian (DST-RFBR) project No. INT/RFBR/P-100 for this work. SBP also acknowledge Dr. Koji S. Kawabata for useful discussions on various polarimetric aspects. C. Eswaraiiah acknowledges the financial support of the Pan-STARRS grant NSC 102-2119-M-008-001 funded by the Ministry of Science and Technology of Taiwan J. Gorosabel acknowledges support of the Unidad Asociada IAA/CSIC-UPV/EHU and the Ikerbasque science foundation. This work has been supported by Spanish Junta de Andalucía through program FQM-02192 and from the Spanish Ministry of Science and Innovation through Projects (including FEDER funds) AYA 2009-14000-C03-01 and AYA2008-03467/ESP. This research has made use of the SIMBAD database, operated at CDS, Strasbourg, France. We acknowledge the usage of the HyperLeda database (<http://leda.univ-lyon1.fr>).

REFERENCES

- Barrett P., 1988, *MNRAS*, 234, 937
- Bayless A. J., Pritchard T. A., Roming P. W. A., et al., 2013, *ApJ*, 764, L13
- Bionta R. M., Blewitt G., Bratton C. B., Casper D., Ciocio A., 1987, *Physical Review Letters*, 58, 1494
- Blondin S., Modjaz M., Kirshner R., Challis P., Berlind P., 2006, *Central Bureau Electronic Telegrams*, 757, 1
- Bose S., Kumar B., Sutaria F., et al., 2013, *MNRAS*, 433, 1871
- Chornock R., Filippenko A. V., Li W., Silverman J. M., 2010, *ApJ*, 713, 1363
- Chugai N. N., 1992, *Soviet Astronomy Letters*, 18, 168
- Chugai N. N., 2006, *Astronomy Letters*, 32, 739
- Clayton G. C., Wolff M. J., Gordon K. D., Smith P. S., Nordsieck K. H., Babler B. L., 2004, *AJ*, 127, 3382
- Cropper M., Bailey J., McCowage J., Cannon R. D., Couch W. J., 1988, *MNRAS*, 231, 695
- Dessart L., Hillier D. J., 2011, *MNRAS*, 410, 1739
- Doi T., Nakano S., Itagaki K., Naito H., Iizuka R., 2007, *Central Bureau Electronic Telegrams*, 848, 1
- Elmhamdi A., Danziger I. J., Chugai N., et al., 2003, *MNRAS*, 338, 939
- Eswaraiah C., Maheswar G., Pandey A. K., Jose J., Ramaprakash A. N., Bhatt H. C., 2013, *A&A*, 556, A65
- Eswaraiah C., Pandey A. K., Maheswar G., et al., 2011, *MNRAS*, 411, 1418
- Eswaraiah C., Pandey A. K., Maheswar G., Chen W. P., Ojha D. K., Chandola H. C., 2012, *MNRAS*, 419, 2587
- Fagotti P., Dimai A., Quadri U., et al., 2012, *Central Bureau Electronic Telegrams*, 3054, 1
- Falk S. W., Arnett W. D., 1977, *ApJS*, 33, 515
- Filippenko A. V., Leonard D. C., 2004, in *Cosmic explosions in three dimensions*, edited by P. Höflich, P. Kumar, J. C. Wheeler, 30
- Folatelli G., Gonzalez S., Morrell N., 2007, *Central Bureau Electronic Telegrams*, 850, 1
- Fraser M., Maund J. R., Smartt S. J., et al., 2012, *ApJ*, 759, L13
- Freedman W. L., Madore B. F., Gibson B. K., et al., 2001, *ApJ*, 553, 47
- Gorosabel J., de Ugarte Postigo A., Castro-Tirado A. J., et al., 2010, *A&A*, 522, A14
- Gorosabel J., Larionov V., Castro-Tirado A. J., et al., 2006, *A&A*, 459, L33
- Grassberg E. K., Imshennik V. S., Nadyozhin D. K., 1971, *Ap&SS*, 10, 28
- Han J., 2009, in *IAU Symposium*, edited by K. G. Strassmeier, A. G. Kosovichev, J. E. Beckman, vol. 259 of *IAU Symposium*, 455–466
- Heiles C., 1996, in *Polarimetry of the Interstellar Medium*, edited by W. G. Roberge, D. C. B. Whittet, vol. 97 of *Astronomical Society of the Pacific Conference Series*, 457
- Heiles C., 2000, *AJ*, 119, 923
- Hirata K., Kajita T., Koshiha M., Nakahata M., Oyama Y., 1987, *Physical Review Letters*, 58, 1490
- Höflich P., 1995, *ApJ*, 440, 821
- Höflich P., 1991, *A&A*, 246, 481
- Höflich P., Khokhlov A., Wang L., 2001, in *20th Texas Symposium on relativistic astrophysics*, edited by J. C. Wheeler, H. Martel, vol. 586 of *American Institute of Physics Conference Series*, 459–471
- Hough J. H., Bailey J. A., Rouse M. F., Whittet D. C. B., 1987, *MNRAS*, 227, 1P
- Immler S., Brown P. J., 2012, *The Astronomer’s Telegram*, 3995, 1
- Itoh R., Ui T., Yamanaka M., 2012, *Central Bureau Electronic Telegrams*, 3054, 2
- Jeffery D. J., 1991, *ApJS*, 77, 405
- Jerkstrand A., Smartt S. J., Fraser M., et al., 2013, *ArXiv e-prints*
- Kasen D., Thomas R. C., Nugent P., 2006, *ApJ*, 651, 366
- Kawabata K. S., Deng J., Wang L., et al., 2003, *ApJ*, 593, L19
- Kawabata K. S., Jeffery D. J., Iye M., et al., 2002, *ApJ*, 580, L39
- Khokhlov A., Höflich P., 2001, in *Explosive Phenomena in Astrophysical Compact Objects*, edited by H.-Y. Chang, C.-H. Lee, M. Rho, I. Yi, vol. 556 of *American Institute of Physics Conference Series*, 301–312
- Kochanek C. S., Khan R., Dai X., 2012, *ApJ*, 759, 20
- Kotak R., Meikle P., Pozzo M., et al., 2006, *ApJ*, 651, L117
- Leonard D. C., Dessart L., Hillier D. J., Pignata G., 2012a, in *American Institute of Physics Conference Series*, edited by J. L. Hoffman, J. Bjorkman, B. Whitney, vol. 1429 of *American Institute of Physics Conference Series*, 204–207
- Leonard D. C., Filippenko A. V., 2001, *PASP*, 113, 920
- Leonard D. C., Filippenko A. V., 2005, in *1604-2004: Supernovae as Cosmological Lighthouses*, edited by M. Turatto, S. Benetti, L. Zampieri, W. Shea, vol. 342 of *Astronomical Society of the Pacific Conference Series*, 330
- Leonard D. C., Filippenko A. V., Ardila D. R., Brotherton M. S., 2001, *ApJ*, 553, 861
- Leonard D. C., Filippenko A. V., Chornock R., Li W., 2002, *AJ*, 124, 2506
- Leonard D. C., Filippenko A. V., Ganeshalingam M., et al., 2006, *Nature*, 440, 505

- Leonard D. C., Pignata G., Dessart L., et al., 2012b, *The Astronomer's Telegram*, 4033, 1
- Li W., Wang X., Van Dyk S. D., Cuillandre J.-C., Foley R. J., Filippenko A. V., 2007, *ApJ*, 661, 1013
- Maund J. R., Spyromilio J., Höflich P. A., et al., 2013, *MNRAS*, 433, L20
- Maund J. R., Wheeler J. C., Patat F., Wang L., Baade D., Höflich P. A., 2007, *ApJ*, 671, 1944
- McCall M. L., 1984, *MNRAS*, 210, 829
- Medhi B. J., Maheswar G., Pandey J. C., Tamura M., Sagar R., 2010, *MNRAS*, 403, 1577
- Mendez M., Clocchiatti A., Benvenuto O. G., Feinstein C., Maraco H. G., 1988, *ApJ*, 334, 295
- Morrell N., Stritzinger M., 2008, *Central Bureau Electronic Telegrams*, 1335, 1
- Munari U., Henden A., Belligoli R., et al., 2013, *New A*, 20, 30
- Munari U., Vagnozzi A., Castellani F., 2012, *Central Bureau Electronic Telegrams*, 3054, 3
- Nakano S., Itagaki K., Kadota K., 2006, *Central Bureau Electronic Telegrams*, 756, 1
- Pandey J. C., Medhi B. J., Sagar R., Pandey A. K., 2009, *MNRAS*, 396, 1004
- Patat F., Höflich P., Baade D., Maund J. R., Wang L., Wheeler J. C., 2012, *A&A*, 545, A7
- Paturel G., Petit C., Prugniel P., et al., 2003, *A&A*, 412, 45
- Pereyra A., Magalhães A. M., Rodrigues C. V., et al., 2006, *A&A*, 454, 827
- Poznanski D., Prochaska J. X., Bloom J. S., 2012, *MNRAS*, 426, 1465
- Ramaprakash A. N., Gupta R., Sen A. K., Tandon S. N., 1998, *A&AS*, 128, 369
- Rautela B. S., Joshi G. C., Pandey J. C., 2004, *Bulletin of the Astronomical Society of India*, 32, 159
- Russell D. G., 2002, *ApJ*, 565, 681
- Scarrott S. M., Rolph C. D., Semple D. P., 1990, in *Galactic and Intergalactic Magnetic Fields*, edited by R. Beck, R. Wielebinski, P. P. Kronberg, vol. 140 of *IAU Symposium*, 245–251
- Scarrott S. M., Rolph C. D., Wolstencroft R. W., Tadhunter C. N., 1991, *MNRAS*, 249, 16P
- Schlegel D. J., Finkbeiner D. P., Davis M., 1998, *ApJ*, 500, 525
- Schmidt G. D., Elston R., Lupie O. L., 1992, *AJ*, 104, 1563
- Serkowski K., Mathewson D. S., Ford V. L., 1975, *ApJ*, 196, 261
- Shapiro P. R., Sutherland P. G., 1982, *ApJ*, 263, 902
- Siviero A., Tomasella L., Pastorello A., et al., 2012, *Central Bureau Electronic Telegrams*, 3054, 4
- Stockdale C. J., Ryder S. D., Van Dyk S. D., et al., 2012, *The Astronomer's Telegram*, 4012, 1
- Tanaka M., Kawabata K. S., Hattori T., et al., 2012, *ApJ*, 754, 63
- Urobin V. P., 2007, *A&A*, 461, 233
- Van Dyk S. D., Cenko S. B., Poznanski D., et al., 2012, *ApJ*, 756, 131
- Van Dyk S. D., Davidge T. J., Elias-Rosa N., et al., 2010, *ArXiv e-prints*
- van Leeuwen F., 2007, *A&A*, 474, 653
- Wang L., Baade D., Höflich P., et al., 2003a, *ApJ*, 591, 1110
- Wang L., Baade D., Höflich P., Wheeler J. C., 2003b, *ApJ*, 592, 457
- Wang L., Howell D. A., Höflich P., Wheeler J. C., 2001, *ApJ*, 550, 1030
- Wang L., Wheeler J. C., 1996, *ApJ*, 462, L27
- Wheeler J. C., 2000, in *American Institute of Physics Conference Series*, edited by S. S. Holt, W. W. Zhang, vol. 522 of *American Institute of Physics Conference Series*, 445–466
- Wheeler J. C., Filippenko A. V., 1996, in *IAU Colloq. 145: Supernovae and Supernova Remnants*, edited by T. S. Kuhn, 241
- Yadav N., Ray A., Chakraborti S., et al., 2013, *ArXiv e-prints*
- Zhang T., Wang X., Li W., et al., 2006, *AJ*, 131, 2245